Aust. J. Phys., 1992, **45**, 193–219

Negative Corona Current Pulses and Cathode Sheath Instabilities in a Short Point–Plane Gap in CO_2

M. Černák[A] *and T. Hosokawa*[B]

[A] Institute of Physics, Comenius University,
Bratislava 842 15, Czechoslovakia.
[B] Department of Electrical and Computer Engineering,
Nagoya Institute of Technology, Showa, Nagoya 466, Japan.
Present address: Department of Electrical Engineering,
Hosei University, Koganei, Tokyo 184, Japan.

Abstract

Waveforms of the first negative corona current pulses have been measured in CO_2 and CO_2+SF_6 mixtures as a function of applied voltage and gas pressure in the range 6·67–66·7 kPa. A complex form of the pulses with a step on the pulse leading edge and a current hump on the pulse trailing part has been found at gas pressures below 40 kPa. Changing the cathode surface material from copper to copper iodide, which has an exceptionally high photoelectric yield, resulted in at least a twofold increase in height of the step on the pulse leading edge, but had little effect on the main current rise to the pulse peak. The use of unconditioned cathodes resulted in the appearance of peculiar current spikes on the pulse tail, which are tentatively attributed to positive-streamer-like instabilities of the cathode sheath. The implications of these results for theories of Trichel pulse formation are discussed, and a physical picture of the phenomenon based on the presumed existence of a cathode-directed streamer associated with the steep pulse rise is outlined.

1. Introduction

When a sufficiently high negative voltage is applied to the point of a point–plane electrode system in an electronegative gas such as O_2, air or CO_2, after a statistical time lag a pulsating corona current of frequency ranging from 10^3 to 10^6 Hz is observed in the external circuit. The pulses immediately following the first one are of lower magnitude and become regular after roughly 10 pulses. These negative corona current pulses were first observed by M. O'Day, but were studied in detail by Trichel (1938) after whom they are named.

At higher gas pressures, above say 20 kPa, Trichel pulses are relatively simple in form, characterized by a fast current rise to a peak value of the order of several mA in a few ns, followed usually by two more gradual exponential falls. At lower gas pressures, Trichel pulses are found to exhibit a more complex form with a step on the leading edge, which is more pronounced with a larger point radii and for the first pulse in a pulse train. The pulse peak is typically followed by a current plateau, which becomes more pronounced as the applied voltage increases.

Recent interest in the experimental study of Trichel pulses has been stimulated by the theoretical work of Morrow (1985*a*, 1985*b*), which has greatly added to the

0004-9506/92/020193$05.00

understanding of the phenomenon. To account for the pulse shape complexity, Morrow's theory invokes two distinct processes which cause the emission of secondary electrons at the cathode, one due to photon impact and the other to positive ion impact. According to the earlier work of Morrow (1985*a*), the presence of secondary electrons due to photoemission leads to a feedback mechanism which sustains the discharge during the steep current rise and initial quenching of the simple-shaped Trichel pulse, with secondary electron emission at the cathode due to ionic impact playing a role only at later times, which corresponds to the pulse trailing part. For the formation of the step on the pulse leading edge observed at lower gas pressures, according to Morrow's later work (1985*b*), after the initial rise in current fed by cathode photoemission, space charge effects lead to a reduction in the electric field near the point and the formation of a cathode sheath, causing a fall in the current. The discharge then begins to be 'externally' maintained by electron emission from the cathode due to incoming ions, and the current begins again to rise rapidly. This rise continues until the number of positive ions in the cathode fall region becomes depleted and the electric field in the region falls, leading to gradual current decay in the pulse trailing part.

This paper is an extension of our previous work (Černák and Hosokawa 1988*a*, 1988*b*, 1989, 1991; Černák *et al.* 1990) and presents the results of measurements of the waveforms of the first Trichel pulses in pure CO_2 and in CO_2 with a small admixture of SF_6, as a function of applied voltage and gas pressure. The measurements were designed to ascertain the validity of Morrow's theoretical proposition regarding pulse shape formation and to provide a basis for modifying and extending the theory. Special emphasis is given here on determining the role played by cathode photoemission in the formation of the pulse shapes. To this end, copper iodide, which has an exceptionally high photoelectric yield, was used as an alternative cathode surface material to copper.

Regarding the question of the formation of the step on the pulse leading edge and pulse development beyond the pulse peak, the experimentally observed current pulses are in general agreement with the predictions of Morrow's theory. However, some experimental results have been found which call for an elaboration of the theory, particularly in the identification of the mechanism responsible for the steep pulse current rise to the pulse peak. An attempt is made in the present paper to consider how the problem of this steep current rise may be approached in terms of a cathode-directed streamer.

2. Experimental Setup and Procedure

The experimental setup used is shown schematically in Fig. 1. The inverted point–plane gap consisted of a hyperbolic capped Cu cathode with a tip curvature radius r_0 and a 50 mm overall diameter stainless steel anode with a 90° Rogowski profile. The grounded cathode was mounted on a movable platform and the point-to-plane spacing $S = 20$ mm was measured to within approximately $0 \cdot 1$ mm. The discharge gap was housed in a stainless steel vessel of 12 L capacity. The operating pressure of the gas was measured by a Baratron gauge with an accuracy better than 2%. The vessel was equipped with a quartz window which could be used to irradiate the discharge gap with UV light from a mercury discharge lamp.

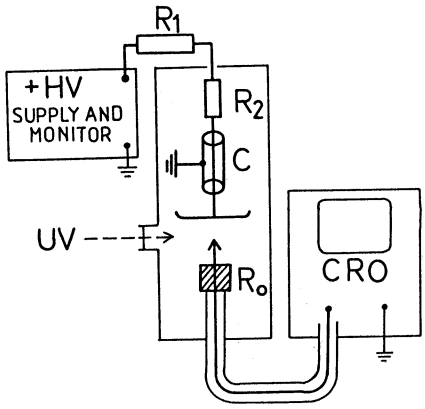

Fig. 1. Experimental arrangement.

A stabilised dc HV supply and monitor were connected to the storage capacitor $C = 1000$ pF via a resistor $R_1 = 10^5\ \Omega$ and a damping resistor $R_2 = 50\ \Omega$. The energy stored in the capacitor was chosen to be of a value insufficient to cause damage to the oscilloscope in case of a spark, but large enough to hold practically constant voltage during the recording of discharge phenomena. Not shown in Fig. 1 is a HV probe which was connected to the anode to check the actual anode potential. To reduce the impedance mismatching between the cathode and detection equipment, which causes ringing on the current traces, a 50 Ω measuring resistor R_0 consisting of six parallel 300 Ω metal-film resistors was placed as near to the cathode tip as possible without perturbation of the electric field at the tip. The optimal value for the distance was determined to be 30 mm. The signal was fed directly, without a feedthrough, by a 50 Ω semiflexible coaxial transmission line to an Iwatsu TS-8123 digital storage oscilloscope and then recorded, using a personal computer to facilitate data manipulation. The RC time constant of the detection circuit was of the order of 0·1 ns. The measurements of the discharge current waveforms were limited by the 100 MHz bandwidth of the Iwatsu storage oscilloscope, corresponding to a rise-time of 3·5 ns.

The experiments were carried out in static CO_2 gas with a purity of 99·9% and in static CO_2+0·1–1% SF_6 gas mixtures. We use the term 'freshly polished' to denote the cathodes polished and washed in acetone to remove loose dirt and oily films. The 'conditioned' cathodes were produced by running a glow discharge in N_2 at 10 kPa and 0·25 mA for 5 minutes in order to obtain a stable cathode surface. To test the role of cathode photoemission we performed experiments using a cathode coated with copper iodide. The 'CuI-coated' cathodes were made by soaking the freshly polished cathodes in a solution of 1 g per litre iodine in acetone for 5 minutes.

Before the start of experiments, the chamber was evacuated to better than 10^{-3} Pa and the CO_2 or CO_2+SF_6 gas mixture was admitted into the system. The cylindrical storage capacitor C was then charged via the resistors R_1 and R_2 to a high positive voltage U. Because the high-field region of the point cathode was so limited in area and volume that there was a large statistical time lag, we initiated the discharge after stabilisation of the potential on the storage capacitor

by a very faint irradiation of the gap with UV light from an 80 W mercury lamp. Thus, an overvoltage as high as 100% could have been applied to the discharge chamber, before discharge ignition by UV light. We note that the intensity of the radiation was just sufficient to ensure initiating electron production. No attempt was made, however, to determine the intensity distribution within the gap.

Even if energy dissipation in the gap during measurements was strictly limited, the chamber was refilled after each series of three discharges. Since the discharge damages the CuI coating on the cathode surface, the coating was renewed after each shot.

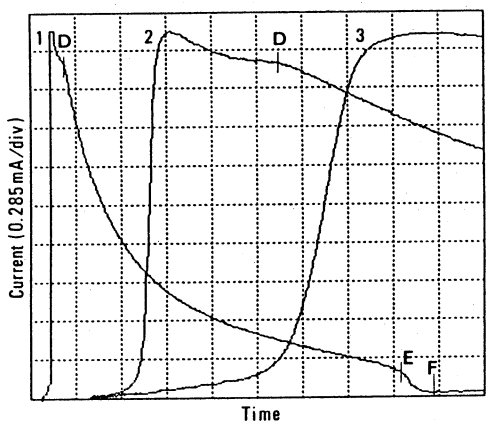

Fig. 2. First Trichel pulse in CO_2 at 6·67 kPa ($r_0 = 0{\cdot}37$ mm, $S = 2$ cm) taken at 2·7 kV (the corona pulse onset voltage with UV irradiation) over the following timescales: (1) 500 ns/div, (2) 50 ns/div and (3) 10 ns/div. Current pulse features at D, E and F are explained in the text.

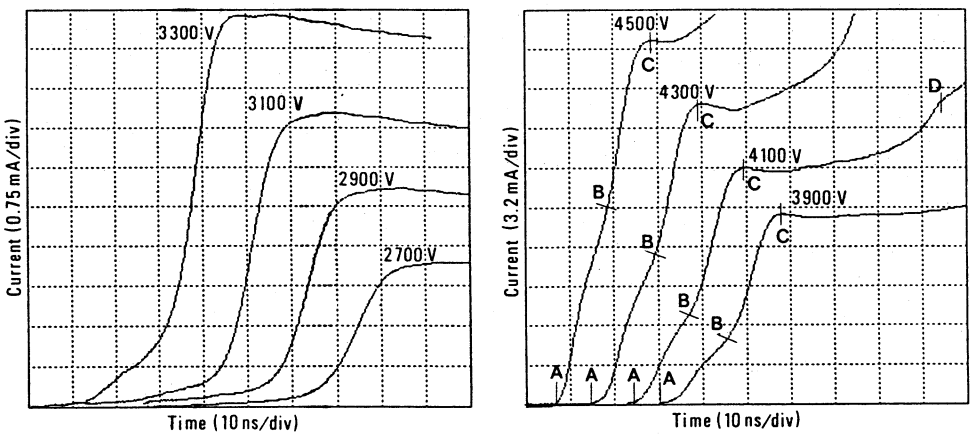

Fig. 3. Development of a current step on the pulse leading edge with increasing gap voltage in CO_2 at 6·67 kPa ($r_0 = 0{\cdot}37$ mm, $S = 2$ cm). The gap voltage is given on the curves. Current pulse features marked by A, B, C and D are explained in the text.

3. Experimental Results

(a) Complex Waveforms of First Trichel Pulses

Under the conditions of these experiments (i.e. relatively blunt cathodes and short discharge gaps), no Trichel pulses occurred in CO_2 at pressures $p < 6{\cdot}67$ kPa. Fig. 2 shows the waveforms of the first Trichel pulses for $p = 6{\cdot}67$ kPa obtained at the pulse onset voltage with UV illumination of $U_0 = 2700$ V over different timescales. Close examination of the pulse waveform (see trace 3) shows that initially the current gradually grew to roughly 7% of the pulse amplitude in some 35 ns, and subsequently rose more steeply to the peak value in the next 30 ns. The pulse maximum was at about 150 ns (see trace 2) followed by a current 'hump' on the pulse trailing part (denoted by D). The hump was followed by two exponential falls (DE and EF) with different time constants.

The development of the waveform features with increasing voltage at a pressure of 6·67 kPa is shown in Figs 3 and 4. Fig. 3 shows that the initial gradual current growth became shorter and steeper as the voltage was increased, which at higher voltage values resulted in the formation of a pronounced step on the pulse leading edge (see the current growth from A to B in Fig. 3*b*). Both the pulse peak current (at point C) and step height (at point B) values increased with increasing voltage, the latter more rapidly. The pulse waveforms were easily reproduced; for example, the pulse amplitudes were repeatable to within roughly 3%.

Fig. 4 shows the development of current growth waveforms with increasing voltage over a longer timescale. At voltages $U > 2800$ V the last exponential current decrease to nearly zero (as seen in Fig. 2, trace 1) was not observed, i.e. the initial peaked current signal corresponding to the Trichel pulse rise and its initial decay was followed by a steady negative glow corona current for roughly $2800 < U < 2950$ V, and by a glow/arc transition at the higher voltage values. The hump (denoted by D) following the initial current peak became more pronounced, and the time lapse between them decreased with increasing voltage.

To illustrate the effect of increasing electron attachment rate on the pulse shape, Fig. 5 shows current growth waveforms for $p = 6{\cdot}67$ kPa and $U = 4$ kV in CO_2 containing small admixtures of strongly attaching SF_6. It can be seen that the first peak current C initially increases slightly with SF_6 concentration, and then decreases progressively with further increase in SF_6 concentration. The presence of SF_6 had a much larger effect on the discharge development beyond the current peak, where it resulted in faster current fall. For SF_6 levels below 0·4%, the current hump D on the pulse trailing part, following the pulse maximum C by 50–70 ns, became more pronounced with increasing SF_6 concentration. The hump was, however, increasingly less pronounced with a further increase in SF_6 concentration and the formation of a second peak (denoted by X), following the main pulse peak by some 200 ns, was observed at a concentration of 0·6%.

Oscillograms taken at a pressure of 13·33 kPa presented in Figs 6–9 show similar trends to the results for 6·67 kPa. Fig. 6, where the current step AB on the pulse leading edge can be seen together with the hump D on the pulse trailing part, illustrates clearly the complexity of the Trichel pulse shape. The increase in gas pressure leads to a significant reduction in the pulse rise time relative to that observed at 6·67 kPa, resulting in the extinction of the

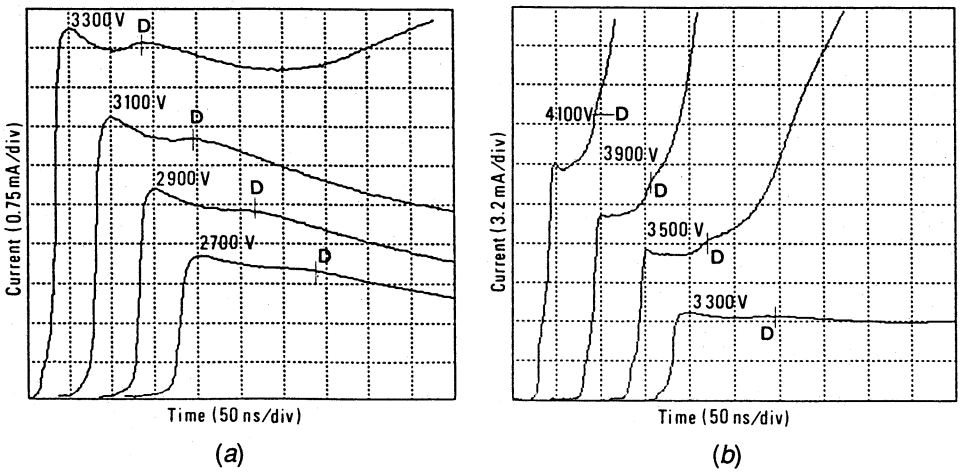

Fig. 4. Development of current pulse waveforms with increasing gap voltage for similar conditions as in Fig. 3 over an expanded timescale. The letter D indicates the hump position.

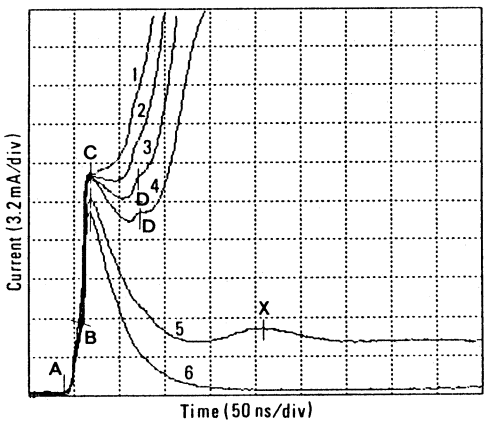

Fig. 5. Effect of adding SF_6 to CO_2 on the pulse waveform at 6·67 kPa and 4 kV ($r_0 = 0{\cdot}37$ mm, $S = 2$ cm). Curves: (1) pure CO_2, (2) CO_2+0·1%SF_6, (3) CO_2+0·2%SF_6, (4) CO_2+0·4%SF_6, (5) CO_2+0·6%SF_6, and (6) CO_2+0·8%SF_6. Current pulse features marked by A, B, C, D and X are explained in the text.

leading edge complex structure at higher voltages, as clearly seen in Fig. 7*b*. An interesting phenomenon is the existence of the peculiar triple-peaked current pulses seen in Fig. 9, observed for SF_6 admixtures between 0·1% and 0·25%.

Returning to Fig. 6, a careful examination of trace 3 reveals that the initial current growth to the step on the pulse leading edge was preceded by low-current (~0·1 mA) precursors. This phenomenon is more readily seen in Fig. 10*a*, where the low-current precursors of the Trichel pulse current rises are shown for ten subsequent discharge shots on an expanded current scale. To circumvent any effect of the UV irradiation, the oscillograms in Fig. 10 were taken at $U = 4600$ V where it was possible to initiate the discharge without UV irradiation with a reasonable lag time between switching on the voltage supply and the arrival of the corona current pulse. It can be clearly seen that for all shots, in order to initiate the first Trichel pulse, it was first necessary to attain a critical current level roughly above 0·05 mA in some 20–100 ns before the steep current rise to

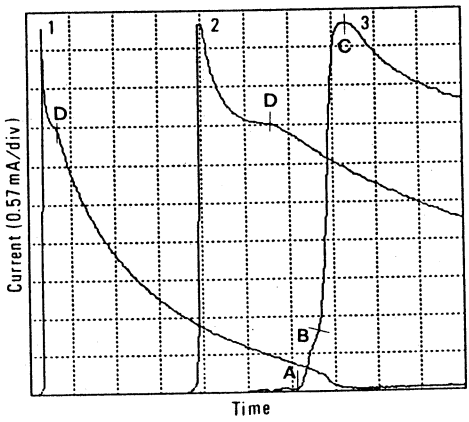

Fig. 6. Complex waveform of the first Trichel pulse in CO_2 at 13·33 kPa taken at 4 kV (the corona pulse onset voltage with UV irradiation) over the following timescales: (1) 500 ns/div, (2) 100 ns/div and (3) 20 ns/div. Current pulse features marked by A, B, C and D are explained in the text.

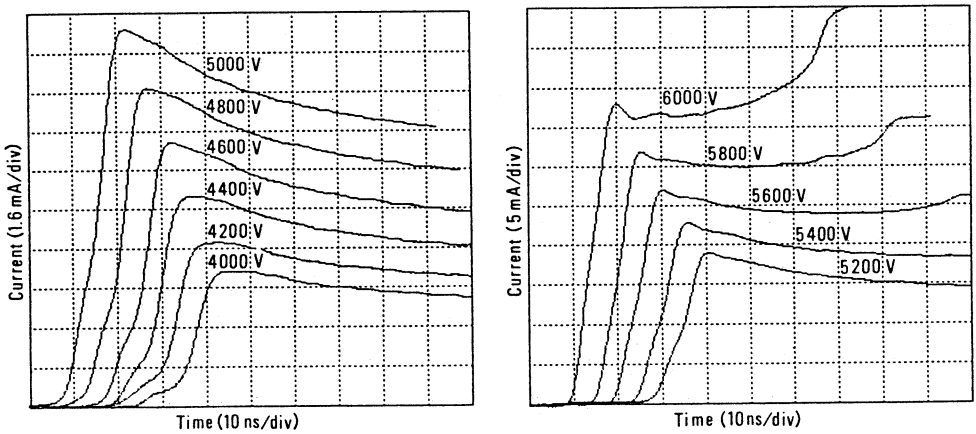

Fig. 7. Development and extinction of the step on the pulse leading edge with increasing gap voltage in CO_2 at 13·33 kPa ($r_0 = 0{\cdot}37$ mm, $S = 2$ cm).

the Trichel pulse. Fig. 10*b* shows similar pre-corona ionisation processes observed under the same experimental conditions which, however, apparently did not result in Trichel pulse onset. In such cases, current maximum was always below 0·05 mA. Although measurements of this phenomenon at other gas pressures and gap voltages have been made, the results are similar in the range of parameters studied and are not presented here.

The first Trichel pulses at a pressure of 40 kPa, shown in Figs 11 and 12, are relatively simple in form. The hump on the pulse tail (marked by D in Fig. 11*a*) was observed only for $U < 5200$ V and, as illustrated in Fig. 12, no complex form of the pulse leading edge was found over the voltage range investigated.

Fig. 13 shows the waveform of the first Trichel pulse in CO_2 at a pressure of 66·7 kPa at the corona onset voltage $U_0 = 4450$ V. The pulse is simple in shape, although a hump is discernible on the pulse trailing part 30–40 ns after the pulse maximum. It can be seen from Fig. 14 that the hump is

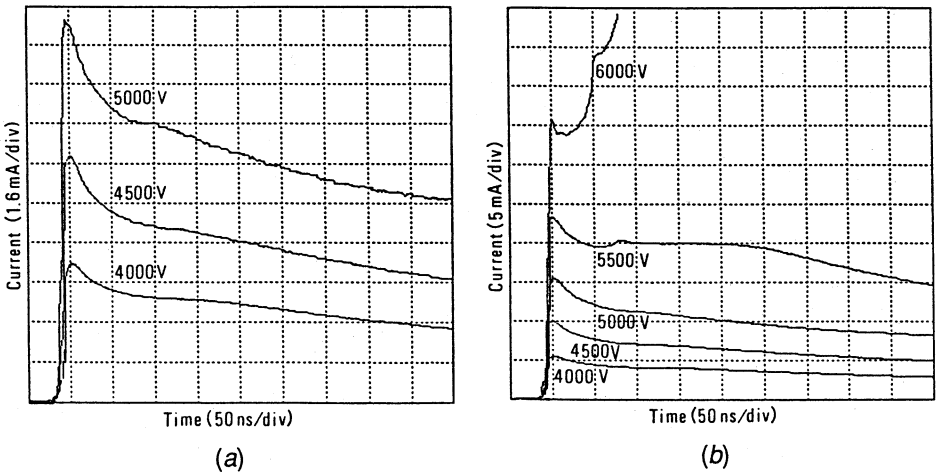

Fig. 8. Development of current pulse waveforms with increasing gap voltage for similar conditions as in Fig. 7, but with expanded timescale.

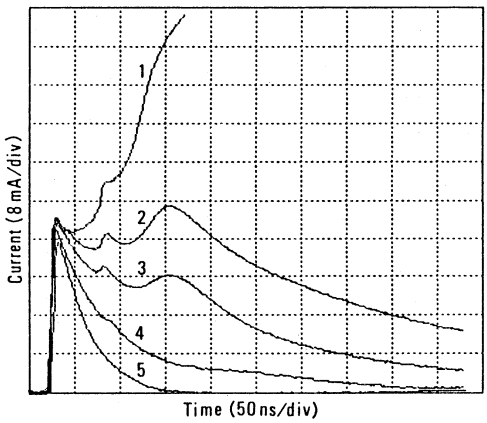

Fig. 9. Effect of adding SF_6 to CO_2 on the pulse waveform at 13·33 kPa and 6 kV ($r_0 = 0{\cdot}37$ mm, $S = 2$ cm). Curves: (1) pure CO_2, (2) CO_2+0·1%SF_6, (3) CO_2+0·25%SF_6, (4) CO_2+0·5%SF_6 and (5) CO_2+1%SF_6.

extinguished for $U > 5000$ V. For pressures higher than 40 kPa, due to the limited time resolution of the oscilloscope used, the recording of the leading edge shape became difficult. Nevertheless, it is noteworthy that no indication of a step on the leading edge was found at 66·7 kPa.

(b) Effect of CuI Coating of Cathode Surface on Pulse Waveforms

As already mentioned in the Introduction, the following investigations were motivated by the fact that when a copper cathode is coated with CuI, the secondary electron photoemission coefficient γ_p usually increases significantly (see Raether 1964). To elucidate also the possible effects of changing the cathode radius, the experiments were performed using two Cu cathodes with minimum radii of curvature $r_0 = 0{\cdot}37$ and $0{\cdot}1$ mm.

Figs 15*a* and 15*b* show waveforms taken for $r_0 = 0{\cdot}1$ mm and $p = 6{\cdot}66$ kPa at the relatively high gap voltage of 4 kV, using the conditioned Cu cathode

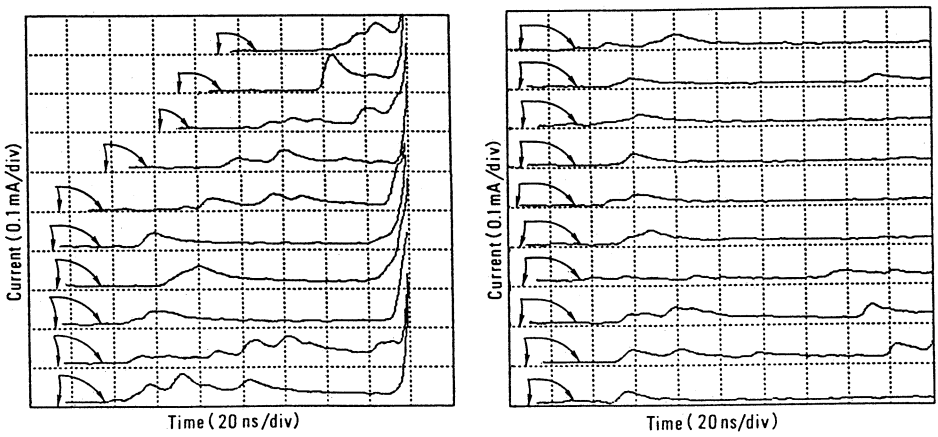

Fig. 10. (*a*) Multi-avalanche/Trichel pulse transitions as indicated by the discharge current growth and (*b*) multi-avalanche current pulses which did not result in Trichel pulse onset, taken in CO_2 at 13·33 kPa and 4·6 kV without UV irradiation ($r_0 = 0{\cdot}37$ mm, $S = 2$ cm). The discharge current traces and corresponding zero current levels are marked with duplex arrows.

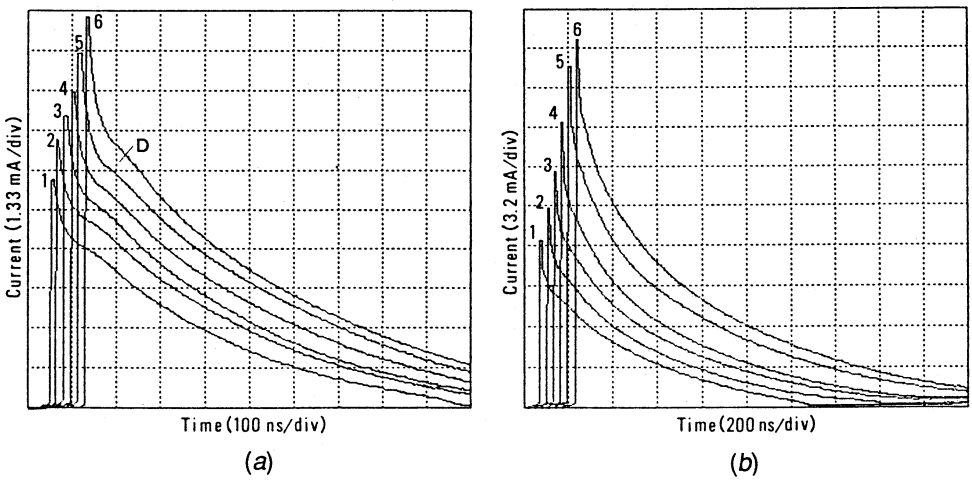

Fig. 11. Development of current pulse waveforms with increasing gap voltage in CO_2 at 40 kPa ($r_0 = 0{\cdot}37$ mm, $S = 1$ cm). Gap voltages in Fig. 11*a*: (1) 4·5 kV, (2) 4·6 kV, (3) 4·7 kV, (4) 4·8 kV, (5) 4·9 kV and (6) 5 kV. Gap voltages in Fig. 11*b*: (1) 5 kV, (2) 5·2 kV, (3) 5·4 kV, (4) 5·6 kV, (5) 5·8 kV and (6) 6 kV.

(trace 1), the CuI-coated cathode (2), and the freshly polished (i.e. unconditioned) Cu cathode (3). It can be seen that the initial peak current signals are identical for the freshly polished and conditioned cathodes. However, when the freshly polished cathode was used, a peculiar current spike beyond the initial peak current signal was frequently observed. For the effect of CuI coating, the results in Fig. 15*a* show that the coating results in roughly a 100% increase in the height of the step on the pulse leading edge (marked by the horizontal short line), whereas the

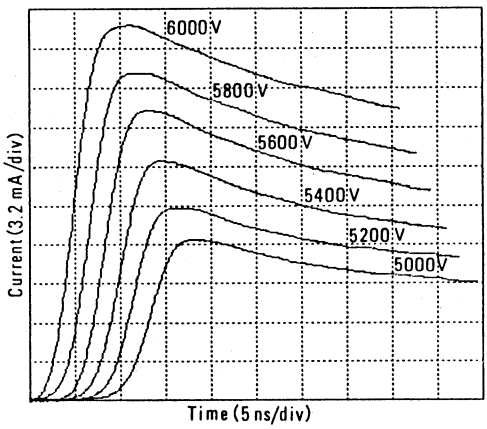

Fig. 12. Pulse leading edges taken for similar conditions as Fig. 11 at the various gap voltages indicated.

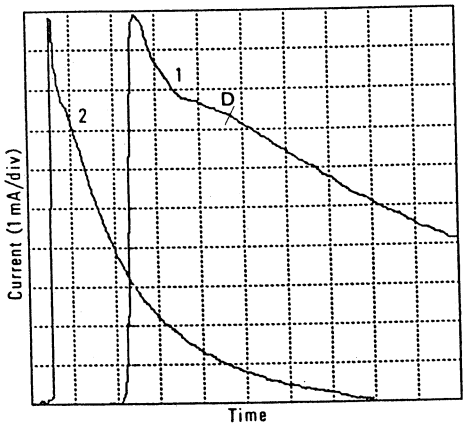

Fig. 13. First Trichel pulse in CO_2 at 66·7 kPa ($r_0 = 0{\cdot}37$ mm, $S = 0{\cdot}5$ cm) taken at 4·45 kV (the corona pulse onset voltage with UV irradiation) over timescales (1) 20 ns/div and (2) 100 ns/div. The letter D indicates the hump position.

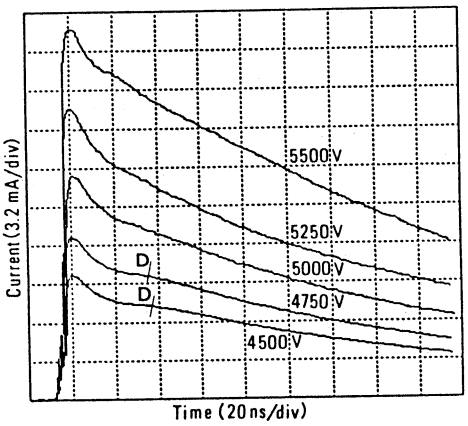

Fig. 14. Development of current pulse waveforms with increasing gap voltage in CO_2 at 66·7 kPa ($r_0 = 0{\cdot}37$ mm, $S = 0{\cdot}5$ cm). The letter D indicates the hump position.

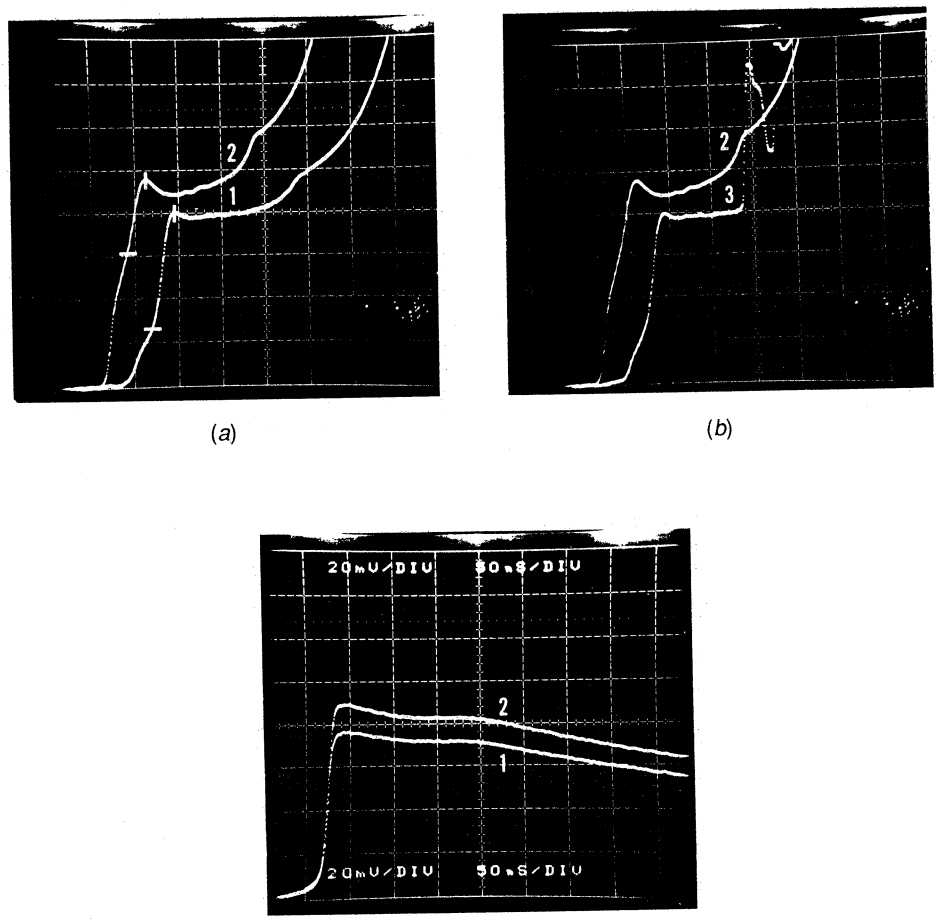

(*a*) (*b*)

(*c*)

Fig. 15. Pulse waveforms in CO_2 at 6·67 kPa taken at various gap voltages (Figs 15*a* and 15*b*—3·9 kV, Fig. 15*c*—2·4 kV) using sharp Cu cathodes ($r_0 = 0{\cdot}1$ mm, $S = 2$ cm) with (1) conditioned, (2) CuI-coated and (3) freshly polished cathodes. Scales: Figs 15*a* and 15*b*—4 mA and 20 ns per division, Fig. 15*c*—0·8 mA and 50 ns per division. Current pulse features marked by the short lines in Fig. 15*a* are explained in the text.

increase in the pulse peak (marked by the vertical line) was only roughly 22%. At the corona pulse onset voltage $U_0 = 1700$ V (see Fig. 15*c*), waveforms for the CuI-coated and conditioned cathodes were remarkably similar, except that the current from the coated cathode was 1·18 times higher. No step on the pulse leading edge was observed in this case.

If the results in Fig. 15 are compared with those in Fig. 16, taken using $r_0 = 0{\cdot}37$ mm, it can be seen that the effect of the CuI coating on current growth at the corona onset voltage is more apparent for the blunt cathode than for the sharp. In particular, CuI coating of the blunt cathode resulted in the formation of a pronounced step on the pulse leading edge, the pulse peak was approximately 38% higher, and the pulse was sharper.

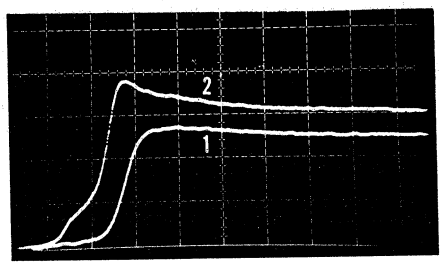

Fig. 16. Pulse waveforms in CO_2 at 6·67 kPa and 2·7 kV (the corona pulse onset voltage with UV irradiation) taken using relatively blunt Cu cathodes ($r_0 = 0{\cdot}37$ mm, $S = 2$ cm) with (1) conditioned and (2) CuI-coated cathode surfaces. Scales: 1 mA and 20 ns per division.

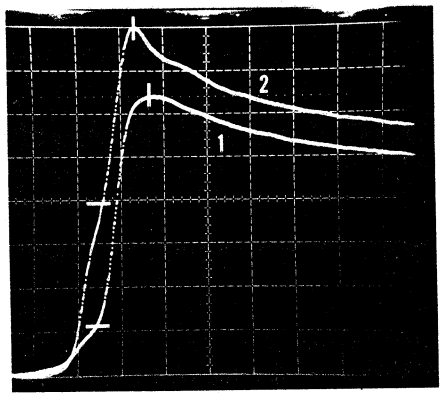

(*a*)

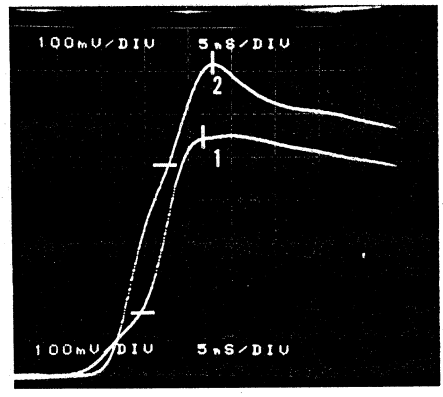

(*b*)

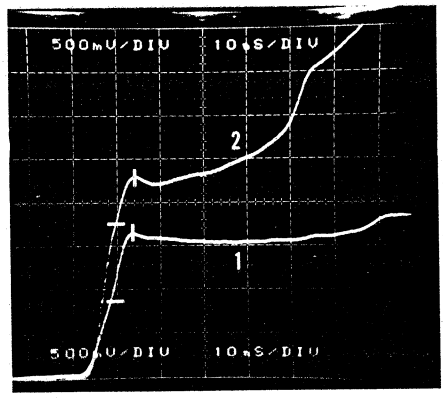

(*c*)

Fig. 17. Pulse waveforms in CO_2 at 13·33 kPa taken at gap voltages (*a*) 4 kV, (*b*) 4·6 kV and (*c*) 5·6 kV, using relatively blunt Cu cathodes ($r_0 = 0{\cdot}37$ mm, $S = 2$ cm) with (1) conditioned and (2) CuI-coated surfaces. Scales: (*a*) 1 mA and 10 ns per division, (*b*) 2 mA and 5 ns per division and (*c*) 10 mA and 10 ns per division. Current pulse features marked by the short lines are explained in the text.

Fig. 17 compares the oscillograms taken using the CuI-coated and the conditioned blunt cathodes at a pressure of 13·33 kPa at various gap voltages. It can be seen that the CuI coating results in a three-fold increase in the step height (marked by the horizontal short line), in a 25–40% rise in the peak current (marked by the vertical line) and, for the lower gap voltages, in a sharper pulse spike. At 5·6 kV (Fig. 17*c*) the pulse spikes were similar in shape and a reduction in the time lapse between the pulse peak and the hump on the pulse trailing part, due to the CuI coating, can be seen. There were no readily detectable differences in the pulse shapes when the fresh and the conditioned cathodes were used, except frequent observations of peculiar spikes riding on the pulse trailing part, similar

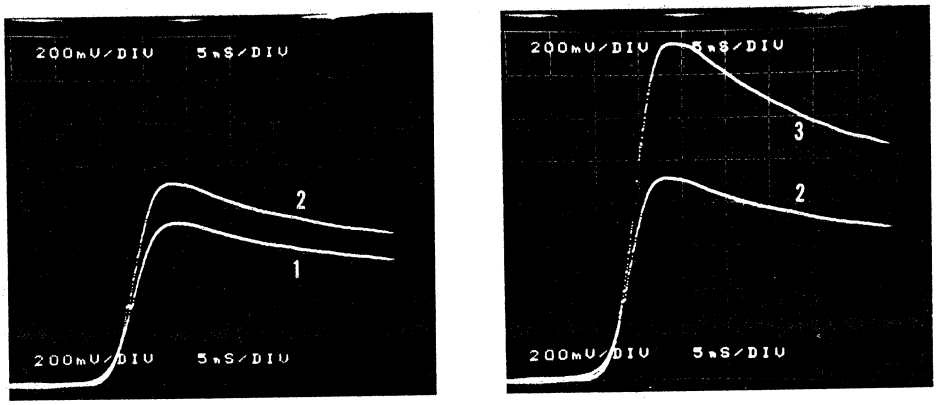

(*a*) (*b*)

Fig. 18. Pulse waveforms in CO_2 at 40 kPa and 5 kV (the corona onset voltage with UV irradiation) taken using relatively blunt Cu cathodes ($r_0 = 0{\cdot}37$ mm, $S = 1$ cm) with (1) conditioned, (2) CuI-coated and (3) freshly polished surfaces. Scales: 4 mA and 5 ns per division.

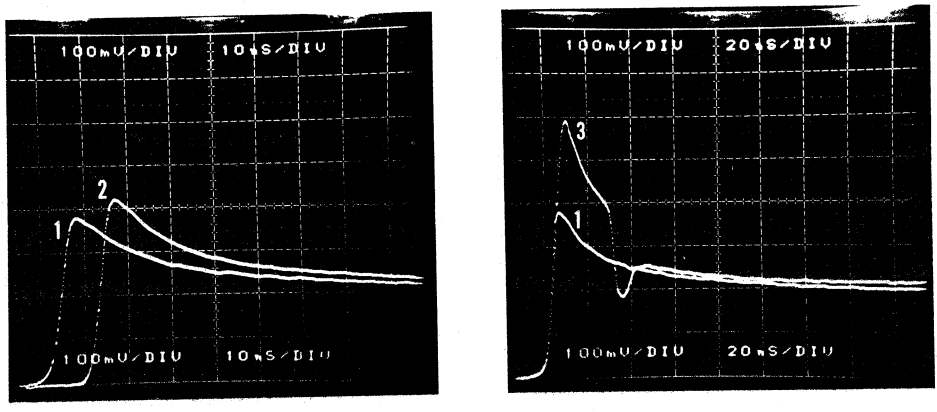

(*a*) (*b*)

Fig. 19. Pulse waveforms in CO_2 at 40 kPa and 6 kV taken using relatively sharp Cu cathodes ($r_0 = 0{\cdot}1$ mm, $S = 2$ cm) with (1) conditioned, (2) CuI-coated and (3) freshly polished surfaces. Scales: (*a*) 2 mA and 10 ns per division and (*b*) 2 mA and 20 ns per division.

to that shown in Fig. 15*b* at a pressure of 6·67 kPa. It must be noted that at 13·33 kPa the pulse characteristics of cathodes conditioned by a low-pressure glow discharge were less reproducible than at lower gas pressures. An acceptable reproducibility in the pulse shape was achieved by allowing the negative corona discharge to run at a current level of 0·05 mA or more for a period of several minutes.

Figs 18 and 19 compare the first Trichel pulse waveforms taken using the corona-conditioned (traces 1), the CuI-coated (2), and the freshly polished cathodes (3) at a pressure of 40 kPa for the sharp and the blunt cathodes respectively. The pulse waveforms of the coated cathodes exhibit relatively high scatter (typically ±15%) in the peak current values. With this in mind, Figs 18 and 19 show that the current peaks for the CuI-coated cathodes were roughly 10–20% higher than those for the conditioned cathodes. Similarly, the pulses from the freshly polished cathodes were not reproducible in that the current traces varied considerably in shape. In general, however, their amplitudes were significantly higher than those of the CuI-coated cathodes. No steps on the pulse leading edges were observed. A comparison of the waveforms at a pressure of 53·3 kPa in Fig. 20 shows very similar discharge behaviour.

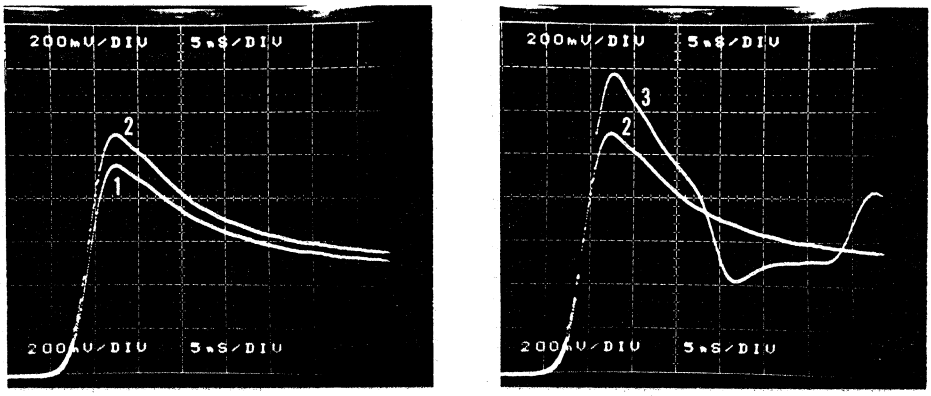

Fig. 20. Pulse waveforms in CO_2 at 66·7 kPa and 5·6 kV taken using relatively sharp Cu cathodes ($r_0 = 0{\cdot}1$ mm, $S = 1$ cm) with (1) conditioned, (2) CuI-coated and (3) freshly polished surfaces. Scales: 4 mA and 5 ns per division.

(c) First Trichel Pulses from Freshly Polished Cathodes

As already indicated in the preceding subsection (see Fig. 15*b*), when the freshly polished cathodes are used, peculiar current spikes riding on the pulse trailing part are observed. Generally, the probability of observing this phenomenon was found to increase with increasing gas pressure. Such current peaks were not observed for $p < 6{\cdot}67$ kPa, but at a pressure of 13·3 kPa they rarely failed to occur, frequently taking the form of quite regular oscillations. For $p > 40$ kPa the spikes often occurred even when the corona-conditioned cathodes were used. At these higher pressures, however, the phenomenon did tend to take place as a sequence of irregular current transients.

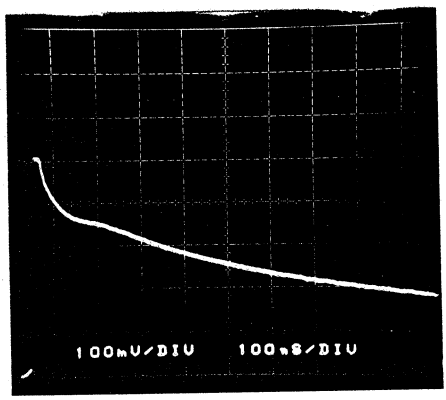

(a)

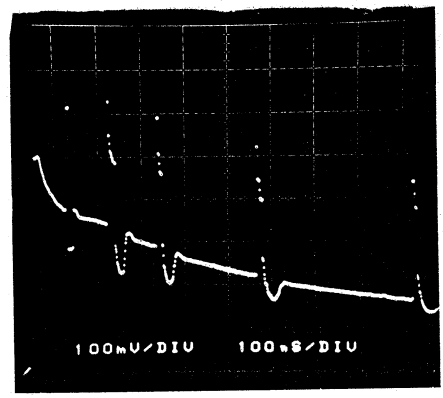

(b)

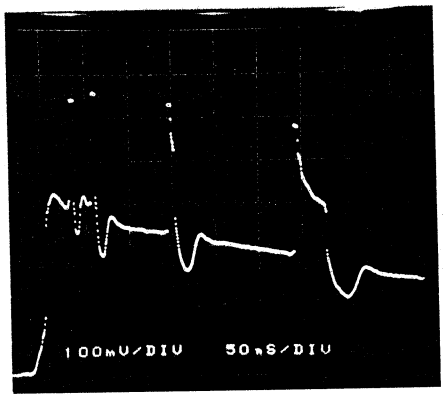

(c)

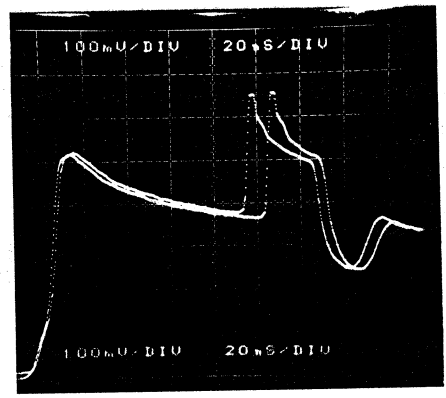

(d)

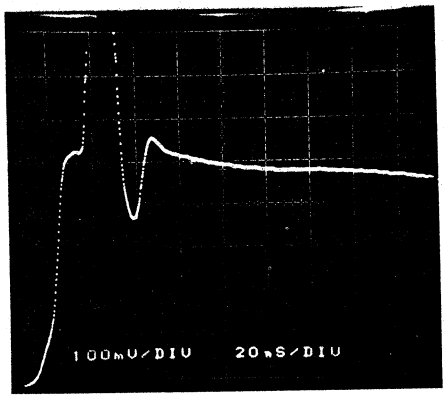

(e)

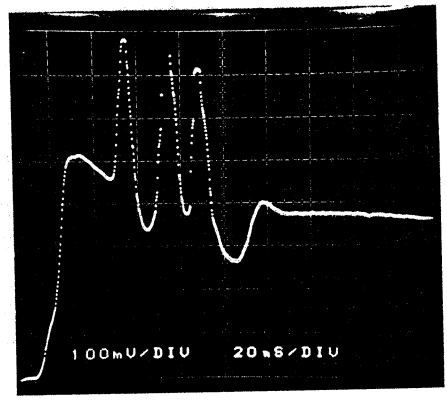

(f)

Fig. 21. Comparison of pulse waveforms taken using (*a*) conditioned and (*b*)–(*f*) freshly polished Cu cathodes ($r_0 = 0{\cdot}37$ mm, $S = 2$ cm) in CO_2 at 13·33 kPa and 4·5 kV. Current scale: 2 mA/div. Timescales: (*a*), (*b*) 50 ns/div, (*d*)–(*f*) 20 ns/div. The waveforms like those in (*d*) using freshly polished cathodes occur with roughly 75% probability.

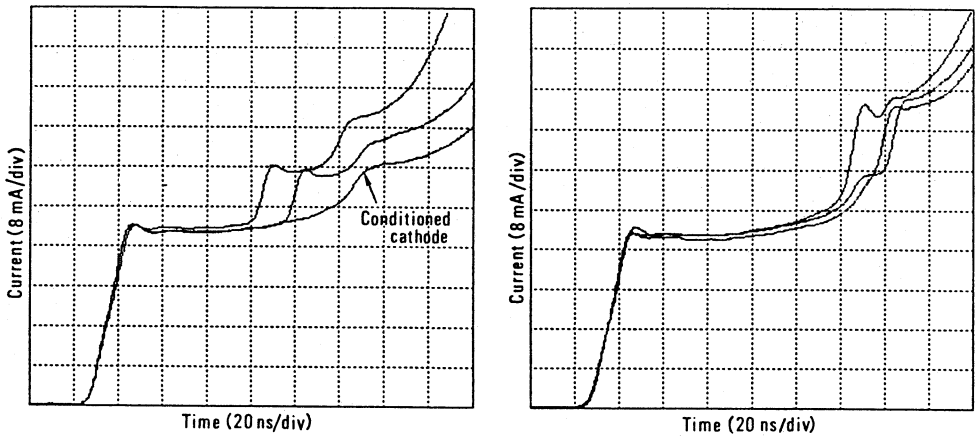

Fig. 22. Comparison of the pulse waveforms taken using conditioned (marked with the arrow) and freshly polished (all other traces) Cu cathodes ($r_0 = 0{\cdot}37$ mm, $S = 2$ cm) in CO_2 at 13·33 kPa and 6 kV.

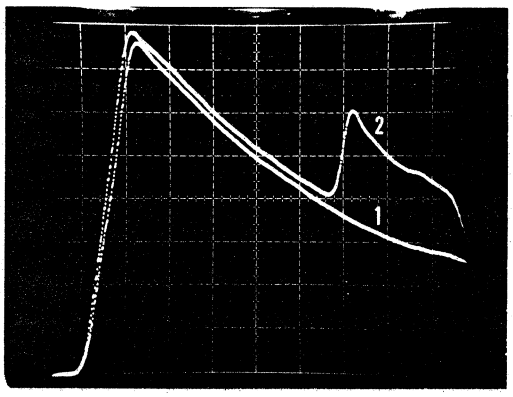

Fig. 23. Comparison of pulse waveforms taken using (1) conditioned and (2) freshly polished Cu cathodes in CO_2+0·2%SF_6 for similar conditions as in Fig. 22. Scales: 4 mA and 10 ns per division.

Fig. 21 compares the waveform of the first Trichel pulse taken at 13·3 kPa using the corona-conditioned cathode with the peculiar first Trichel pulse shapes from the freshly polished cathodes shown over different timescales. Despite an apparent variety in the shapes, the phenomenon was reproducible in that waveforms like those in Figs 21*b* and 21*d* occurred with roughly 75% probability. The first 'peculiar' current spike did tend to take place roughly at the same time after the pulse maximum as the current hump on the trailing part of the first Trichel pulse from the conditioned cathode (see Fig. 21*a*). This trend is clearly seen in Fig. 22, where the hump is more pronounced (see the arrow). Figs 21*e* and 21*f* show a different manifestation of the phenomenon in the form of very sharp current spikes, observed with roughly 10–20% probability.

When re-examining the results in Fig. 21 taken at the corona onset voltage, we can make the following important points:

(i) The height of the spikes riding on the Trichel pulse trailing part and the Trichel pulse at the onset voltage (see e.g. Fig. 7*a*) are nearly equal.

(ii) Each of the spikes is followed by a dip, where the current falls slightly below the common Trichel pulse tail level, being followed by a current peak remarkably similar in shape to the top part of the Trichel pulse.

(iii) The time lapse between the spikes (see Figs 21*b* and 21*c*) tends to decrease with the current level of the Trichel pulse. At higher gap voltages the 'peculiar' spikes exhibit remarkable similarities in shape with the first Trichel pulse spikes, as illustrated by Figs 22 and 23.

4. Discussion

(a) Discussion of Pulse Waveforms in Terms of Morrow's Theory

Considering the fact that interest in the experimental study of Trichel pulses has recently been increased by the theoretical work of Morrow, an attempt is now made to discuss the above results in terms of this theory. It is important to note that the theory has been presented in two papers. In the earlier paper (Morrow 1985*a*), a general theory of the pulsed negative corona was outlined, which claims to explain most features of the simple-shaped Trichel pulses. In the later paper, Morrow (1985*b*) used the same computer model 'with minimal changes in certain parameters to values which are well within the published range' to simulate the development of the step on the leading edge of the first Trichel pulse. Accordingly, both works of Morrow are based on the same theoretical propositions.

Firstly, we discuss the stepped form of the pulse leading edge seen in Figs 3, 6 and 7 in Section 3*a* and Figs 15–17 in Section 3*b*. Such a discharge current growth in a 'step–peak' sequence is apparently analogous to the complex form of the pulse leading edge observed in O_2, which was the subject of the later theoretical study of Morrow (1985*b*). It was proposed that the step–peak sequence of the current growth is due to the difference in arrival times at the cathode of the photons and positive ions produced in the same ionisation region at the same time. Thus, the initial current rise to the step, like that clearly seen in Fig. 3*b*, is proposed to be due to the discharge being fed by secondary electrons ejected from the cathode by photons from excited atoms in the discharge (γ_p emission). Subsequently, this initial current rise is interrupted when sufficient plasma is produced in front of the cathode to reduce the electric field inside the plasma region, forming a rapidly shrinking cathode fall region. Thus, the initial current rise ceases, owing to a reduction in the width of the cathode sheath. However, when positive ions formed at the same time as the photons reach the cathode, since γ_i emission (i.e. the secondary electron emission at the cathode due to ionic impact) is far more effective than γ_p emission, the current rise is enhanced again. The discharge current continues to rise until the number of positive ions in the cathode fall region begins to be depleted. Thus, the current has reached the peak value and begins to fall.

With regard to the question of the secondary emission mechanism active during the formation of the step on the pulse leading edge, our comparison (Černák and Hosokawa 1988*b*) of the current growth in a negative point–plane gap in pure N_2 with that in N_2+90%CH_4, where γ_p emission is suppressed because of the highly

efficient quenching of nitrogen excited states by methane molecules, substantiates Morrow's proposition regarding the crucial role of γ_P emission. Now, further evidence for this proposition comes from the results in Figs 15–17 where, in a striking correspondence with the conclusions of Morrow (1985*b*), the CuI coating of Cu cathodes results in a conspicuous increase in both the current growth rate during the step formation and the step height.

From this discussion of the step–peak sequence in terms of Morrow (1985*b*) it follows that, if the step formation is due to γ_P emission, then the extinction of the stepped form of the pulse leading edge at higher gap voltages (seen in Fig. 7*b*) can only be explained as resulting from the nearly coincident (within some 5 ns) arrival of the photons and ions produced in the same ionisation region at the same time. It is believed, however, that it would be unlikely for the positive ion's space charge to move fast enough to reach the cathode at approximately the same moment as photons, and to be neutralised after several ns. Note that a similar extinction of the stepped form of the pulse leading edge was observed in pure N_2 (Černák and Hosokawa 1988*a*), N_2+30%SF_6 (Černák and Hosokawa 1989) and CO (Černák and Hosokawa 1991). An additional deficiency of the later Morrow work is that it does not provide any explanation of the later stages of pulse development, especially the current hump following the step–peak sequence by 50–100 ns (see Figs 4, 6 and 7*b*). Note that a similar inadequacy of this theoretical work in explaining the later stages of pulse development has been noted by Scott and Haddad (1987).

Now, independent of the above discussion on the stepped form of the pulse leading edge, we turn our attention to the simple-shaped pulse shown in Fig. 2, which is characterised by a peak–hump sequence in the discharge current development. Despite the differences in geometry and gas, this pulse shape is remarkably similar to the pulse shape for O_2 at the same gas pressure measured by Bugge and Sigmond (1969) and simulated numerically in the earlier work of Morrow (1985*a*, see Fig. 1 there) in that:

(i) After an initial slow growth, the current rises sharply, increasing from 10% to 90% of its peak value in 11 ns and 18 ns for O_2 and CO_2 respectively.

(ii) The current peak is in about 100 ns followed by a current hump. Although in the case of the pulse computed for O_2 the hump is less pronounced because the pulse quenching due to electron attachment was rapid, the computations where the electron attachment was set to zero (see Morrow 1985*a*, Fig. 11) illustrate the existence of the peak–hump sequence very well.

Note that both above-mentioned waveforms are also remarkably similar in shape to the waveforms, shown in Figs 8*a*, 11*a*, 13 and 14, taken at higher gas pressures.

The similarity between the later stages of the measured and computed pulse waveforms (see Fig. 6 of Morrow 1985*a*) suggests that, following the current rise and initial quenching phases, the discharge is maintained by γ_i emission, causing the formation of the hump on the pulse trailing part. It can be added that Morrow (1985*a*) also offered a very plausible explanation for the peculiar triple-peaked pulses in Fig. 9. So, we believe that the apparent similarity between the triple-peaked pulses in Fig. 9 and the oscillating current growth in Fig. 11 of Morrow (1985*a*) indicates that the results in Fig. 9 are a striking manifestation

of Morrow's proposal of damped current oscillations, reflecting the back and forth motion of the electric field in the cathode fall region. Morrow's earlier computations, explaining the later stages of discharge development in terms of γ_i emission, are also in general agreement with the measurements of the pulse shapes by Scott and Haddad (1987) and the results of Amin (1954). It follows then that Morrow's (1985*a*) earlier computations give useful predictions regarding the role played by γ_i emission in the later stages of pulse development which agree with experiment.

With regard to the question of pulse peak formation, according to Morrow (1985*a*), the presence of secondary electrons due to γ_p emission leads to a feedback mechanism which sustains the discharge during the current rise and initial quenching phase. It is interesting to note that even though there seems to be a consensus that γ_p emission plays a crucial role in steep pulse rise (see e.g. Loeb 1965; Goldman and Goldman 1978), no detailed experimental study has so far been performed on the effect of changing the cathode material on the pulse waveforms, thus leaving some doubt as to the actual mechanism of the steep rise. The only attempt at a rigorous determination of the effect of cathode material, as far as we are aware, is the work of Miyoshi *et al.* (1964) where, surprisingly, the influence of cathode material on Trichel pulse characteristics was found to be insignificant.

For the experimental conditions reported here, the CuI coating resulted in a significant increase in γ_p emission, which is clearly evident from the increase in the current growth rate during the formation of the step on the pulse leading edge at the lower gas pressures, as seen in Figs 15*a*, 16 and 17. However, for higher gas pressures, where the stepped form was not observed, CuI coating of the cathode surface did not substantially alter the pulse waveform, resulting in only about a 20% increase in the pulse maximum, without any change in the pulse rise time, as can be seen in Figs 18*a* and 20*a*. Consequently, these results have cast doubt on whether γ_p emission plays such a crucial role in the steep pulse current rise, as proposed by Morrow (1985*a*). Moreover, we believe that Morrow's theory does not explain why the use of unconditioned cathodes, which for these experiments have apparently the same value of γ_p as conditioned cathodes (compare the steps on the waveforms 1 and 3 in Figs 15*a* and 15*b*), has such a marked effect on the pulse shape at higher gas pressures, as shown in Figs 18*b*, 19*b* and 20*b*.

Our contention that γ_p emission does not play a crucial role in the steep current rise of the simple-shaped pulses is further supported by our unpublished results, comparing the waveforms in N_2+10%Ar and N_2+10%CH_4 gas mixtures, whose α coefficients are roughly equal. For example, for $p = 40$ kPa and $r_0 = 0{\cdot}37$ mm, the pulse amplitude in N_2+10%CH_4 was found to be higher than that in N_2+10%Ar by approximately 14%, despite an approximately six-fold reduction of γ_p in N_2+10%CH_4 compared with that in N_2+10%Ar.

To sum up, the foregoing discussion leads to the following inference: For Morrow's (1985*b*) later work dealing with the step–peak sequence, a large body of experiments shows conclusively that the step on the pulse leading edge is indeed due to γ_p emission. However, the results cast doubt on whether the subsequent current rise to the pulse peak is in fact due to γ_i emission, and Morrow's work provides no explanation for the later stages of pulse development, with particular

reference to the hump on the pulse trailing part. By contrast, the earlier work of Morrow (1985*a*) gives useful predictions regarding the role of γ_i emission in the later stage of pulse development, with particular reference to the hump on the pulse trailing part. However, the proposition of the crucial role of γ_p emission in the steep current rise to the pulse peak seems to be questionable, and Morrow (1985*a*) provides no explanation for the appearance of the step on the pulse leading edge.

Now, it is of interest to discuss here the complex pulse shape shown in Fig. 6, where the step–peak sequence (see trace 3) and the peak–hump sequence (see trace 2) occur simultaneously. Apparently, both Morrow's works taken together provide a very plausible explanation for the step on the pulse leading edge and the hump on the pulse trail, in terms of γ_p and γ_i emission respectively. It follows then, however, that the theory as a combination of both works provides discordant inferences regarding the secondary emission mechanism active during the formation of the pulse peak. This results from the fact that both the step–peak and the peak–hump sequences are claimed to result from the succession of independent γ_p and γ_i emission processes. Therefore, we suppose that the simultaneous occurrence of the step–peak and peak–hump sequences indicates that the actual mechanism for the formation of the pulse peak differs from both γ_i and γ_p based mechanisms suggested by Morrow. Note that the complex step–peak–hump waveforms were also observed in N_2+30%SF_6 (Černák and Hosokawa 1989), CO (Černák and Hosokawa 1991) and in air (our unpublished results).

(b) Concept of Cathode-directed Streamer Associated with Trichel Pulse Rise

Computations aimed at understanding the development of Trichel pulses have been carried out for a number of years (Alexandrov 1963; Ogasawara 1966; Graf 1979 and 1980; Salasoo *et al.* 1985). What is common to them is that they assume γ_p emission to be the main feedback mechanism during the steep pulse current rise to pulse maximum. Since, in principle, the discharge current growth as a succession of electron avalanches linked through γ_p emission feedback to the cathode is embodied in all of them, these models imply that the rate of the pulse current rise is critically dependent on the values of γ_p assumed. This is, however, in contrast to the previously discussed results shown in Figs 18–20.

As a result, in agreement with the conclusions of Morrow's later work on the formation of the step on the pulse leading edge and with the results in Figs 15*a*, 16 and 17, we believe that the approach based on the assumed crucial role of γ_p emission in the discharge current growth corresponds to the current rise to the step on the pulse leading edge, rather than to the steep current rise of the simple-shaped Trichel pulses at higher gas pressures. Therefore, it is logical to call attention to the concept of a cathode-directed primary streamer associated with the steep Trichel pulse rise which, as an alternative to the above-mentioned computational investigations and in conformity with the results in Figs 18–20, neglects the role of secondary electrons produced at the cathode in the steep pulse rise. This concept was first put forward by Ushita *et al.* (1967), and over the two past decades has reappeared in several publications which are discussed below in the context of the present experimental results with the aim of providing further

arguments in favour of the streamer-based concept of Trichel pulse development.

First, it is useful to outline an illustrative picture describing the basic features of the buildup of the streamer sequence, which is based on recent literature reports (see e.g. Hodges *et al.* 1985; Kunhardt and Tzeng 1988). At a certain stage in a sequence of avalanches linked by cathode secondary electron emission, the space charge generated can partially shield itself from the applied field, creating a streamer initiating plasma (estimated to occur when the total number of positive ions produced achieves a critical value of 10^7–10^8). The space charge required for the shielding causes a field enhancement in front of the streamer initiating plasma. If a few electrons are just in front of the plasma, avalanching in the locally enhanced field can cause a primary streamer to propagate. Thus, the feedback-to-cathode Townsend ionisation mechanism is supplanted by a faster feed-forward-to-gas streamer mechanism. The primary streamer can be viewed as an ionising-potential wave characterised by the fact that the background gas is initially nearly neutral. The streamer front propagates with typical velocities 10^7–10^8 $\mathrm{cm\,s^{-1}}$, which is really a phase movement, and can easily be much faster than the charged particles it contains.

For the Trichel pulse mechanism, it seems to be generally accepted (see e.g. Goldman and Goldman 1978) that the spatio-temporal evolution of the field distortion during the pulse rise bears a certain resemblance to the mechanism of advance of the primary cathode-directed streamer in a positive point–plane gap. This hypothesis is corroborated by a detailed spatio-temporal analysis of the luminous phenomena during Trichel pulse development by Ushita *et al.* (1967, 1968) and Ikuta and Kondo (1976). In particular, for the Trichel pulse in air it has been shown that a glow, which can be associated with a streamer-like ionisation wave owing to the simultaneous presence in the emission of the second positive and first negative systems of the nitrogen molecule, is formed at a certain distance from the cathode point and propagates toward it.

According to Goldman and Goldman (1978), the rapid growth of the Trichel pulse current overlaps the propagation of the streamer toward the cathode, reaching the peak current value just as the streamer contacts the cathode. Support for this inference comes from our recent comparisons (Černák *et al.* 1990; Černák 1990) of Trichel pulses with current pulses induced by primary streamers when they contact the cathode in a positive point–plane gap in air, where both phenomena were found to exhibit remarkable similarities. For example, when the pulse peak values were matched by a proper choice of gap voltages, the measured current rise rates were the same, and the initial current peaks were in both cases followed by a filamentary glow discharge phase of the same current level. The proposal of a common mechanism for both the streamer/cathode interaction in a short positive point–plane gap and the Trichel pulse is corroborated also by similar results for CO_2 presented in an Accessory Publication.*

Following this line of reasoning, the recent experiments of Inoshima *et al.* (1990), using CuI coating in a short positive point–plane gap, show that the coating has no perceptible effect on the waveforms of the pulses generated during the neutralisation of the primary streamers at the cathode. This is in apparent correspondence with the modest effect on the Trichel pulse waveforms in Figs 18,

* Available from the authors on request.

19 and 20 and emphasises further the analogy between the simple-shaped Trichel pulses and the current pulses generated during the streamer neutralisation on the cathode.

As suggested by Goldman and Goldman (1978), further support for the streamer-like mechanism of Trichel pulse development is to be found in experimental investigations by Hosokawa *et al.* (1969, 1970), which showed that the transition from pre-corona multi-avalanches to the Trichel pulse occurs when the discharge current reaches a critical level of 0·06 mA and the number of positive ions created by avalanches gives rise to the critical field for initiation of a streamer. The critical current level measured by Hosokawa *et al.* agrees well with the results in Fig. 10, however, the concept of a critical number of positive ions associated with the multi-avalanche/Trichel pulse transition has more physical relevance. Since for the conditions in our experiments the positive ion transit time has been assessed to be some 100–200 ns, as a first approximation, the number of positive ions accumulated at pulse onset may be estimated by considering the time integral of the current traces in Fig. 10*a* up to the steep pulse current rise. From this estimate we may find that the number of positive ions accumulated at the pulse onset is of the order of 10^7. This number is in a suggestive correspondence with the net charge in the streamer head of 10^7–10^8 positive ions typical of streamer calculations. It is noteworthy also that the multi-avalanche/Trichel pulse transitions in Fig. 10*a* closely resemble the multi-avalanche/positive-corona-streamer transitions observed by McAllister *et al.* (1979) and Crichton and Williams (1983). Analogies between the onset of negative corona Trichel pulses and positive corona streamers have been found also by Poli (1982), and by Gallimberti and Marchesi (1982) who have argued that: 'The threshold voltage for both positive and negative (corona) polarities can be defined as the minimum voltage allowing an avalanche, growing in the most favourable conditions, to reach a critical size that can ensure self-sustained streamer propagation.'

Finally, we note the paper by Golinski and Grudzinski (1986) where a statistical analysis of the charge and the light emission of Trichel pulses led the authors to hypothesise that: 'The development of the preliminary avalanche ionisation is stopped owing to the feedback effect of the field due to the negative space charge produced by this ionisation. At the same time, conditions arise permitting the development of an inverse discharge directed from the positive space charge to the point and supported by photo-ionisation. The fronts of the measured Trichel pulses correspond to this discharge and the main part of the light due to Trichel pulses is emitted during it.'

The arguments given above, some of which are still speculative whereas others have been fairly well tested, indicate many points of similarity betwen the initial stages of Trichel pulse formation and the primary streamer/cathode interaction in a short positive point–plane gap. Therefore, we believe that there are many reasons for further examination and study of the Trichel pulse phenomenon in terms of a primary-positive-streamer-like mechanism.

(c) Physical Mechanism for Spikes on the Trichel Pulse Trailing Part

In this subsection an attempt is made to elucidate the physical mechanism responsible for the formation of peculiar current spikes on the Trichel pulse

trailing part, shown in Figs 15*b*, 21, 22 and 23, which were observed using freshly polished cathodes. It is important to emphasise that these current spikes differ from the triple-peaked current pulses in Fig. 9, explained in terms of Morrow's theory in Section 4*a*. This is clearly seen from Fig. 22*a*, where the γ_i induced hump (marked with the arrow) corresponding to the second peak of the triple-peaked pulses in Fig. 9, is shown together with the peculiar current spikes.

As can be seen from Figs 15*b*, 21 and 22, the first peculiar current spike tends to take place roughly at the same time as the current hump on the pulse trailing part. This leads us to the following consideration: As already stated, Morrow's (1985*a*) computations gave useful predictions regarding the later stages of Trichel pulses. According to the computations (compare Figs 1, 2*a* and 5 of Morrow 1985*a*), the field in the immediate vicinity of the cathode passes through its maximum value just as the positive ions responsible for the hump formation are reaching the cathode surface. It is known from studies on CO_2 lasers at near-atmospheric pressures that a cathode-sheath instability, which could be envisaged as a 'breakup' of the cathode sheath (see Turner 1981), tends to take place in times of the order of 1–10 ns after the cathode sheath establishment, resulting in cathode spot formation. If such a cathode-sheath instability also takes place during the later stages of the Trichel pulse, corresponding to an abnormal glow discharge phase, then one would expect that this could come about at the moment when the field in the cathode sheath is passing through its maximum value and the current hump is generated. One can therefore speculate that the current spikes on the pulse tail seen in Figs 15*b*, 21, 22 and 23 can be explained in terms of a cathode-sheath instability. This is supported by the fact that both the cathode-sheath instabilities (Turner 1981) and the spikes tend to occur with unconditioned cathodes.

An insight into this phenomenon can be obtained by considering Figs 22 and 23, where some similarity in shape between the spikes and the initial current rise and following fall of the Trichel pulse can be seen. Note that this similarity is more clearly demonstrated in our recent paper (Černák *et al.* 1990, see Fig. 2), where the phenomena were studied in air. Also, it is noteworthy that Golinski and Grudzinski (1986), in line with other authors (see Loeb 1965, pp. 305–6), have found a sufficiently intense Malter emission of electrons from cathode surface imperfections, such as oxide layers or deposited particles, to allow a Trichel pulse to occur. Apparently, this is a further common point between the Trichel pulse and the spikes observed using freshly polished cathodes with a very high density of surface imperfections. Hence, on the basis of these similarities, it seems reasonable to suppose that the physical mechanism for the spikes in Figs 15*b*, 21, 22 and 23 has much in common with that of the initial stages of the Trichel pulse. Thus, keeping in mind the streamer-based concept for Trichel pulse development in Section 4*b*, we can advance a hypothesis that the peculiar current spikes are due to local positive-streamer-like breakdowns of the cathode sheath.

Note that our related experiments discussed in the Accessory Publication have revealed current spikes analogous to those in Figs 15*b*, 21 and 22 taking place during a filamentary glow discharge phase following the arrival of the primary streamer on the cathode in a short positive point–plane gap. Since these spikes

5. Summary

Waveforms of the first negative corona Trichel pulse have been measured in a short negative point–plane gap as a function of gas pressure, applied voltage and cathode surface state. It was demonstrated that Morrow's (1985*a*, 1985*b*) theory provides a very plausible explanation for the appearance of a step on the pulse leading edge and a hump on the pulse tail in terms of independent photon and ion secondary processes at the cathode. However, at pressures above say 30 kPa, the characteristics of simple-shaped pulses were found to be relatively insensitive to changes in γ_p, which appears to contradict the theory proposed by Morrow. This theory also fails to explain the appearance of complex step–peak–hump pulse waveforms, and provides no explanation of peculiar current spikes on the pulse tail observed using unconditioned cathodes.

To remedy these shortcomings an attempt has been made to extend the theory by invoking a cathode-directed streamer to produce the steep current rise to the Trichel pulse peak. The proposed physical picture has much in common with the model of a cathode-directed ionising-wave-driven cathode-sheath instability due to Bityurin *et al.* (1989*a*, 1989*b*).

References

Alexandrov, G. N. (1963). *Zh. Tekh. Fiz.* **33**, 223–30.
Amin, M. R. (1954). *J. Appl. Phys.* **25**, 627–33.
Bityurin, V. A., and Kulikovski, A. A. (1989*a*). Proc. 19th Int. Conf. on Phenomena in Ionised Gases, Belgrade (Ed. M. J. Labat), pp. 106–7 (University of Belgrade).
Bityurin, V. A., Kulikovski, A., and Lyubimov, G. A. (1989*b*). *Zh. Tekh. Fiz.* **59**, 50–65.
Bugge, C., and Sigmond, R. S. (1969). Proc. 9th Int. Conf. on Phenomena in Ionised Gases, Bucharest, p. 289 (Editura Acad. Republ. Soc. Romania).
Černák, M. (1990). Eighth Symp. on Elementary Processes and Chemical Reactions in Low Temperature Plasma, Stará Lesná (Ed. M. Morvová), pp. 137–55 (Comenius University: Bratislava).
Černák, M., and Hosokawa, T. (1988*a*). *Appl. Phys. Lett.* **52**, 185–7.
Černák, M., and Hosokawa, T. (1988*b*). *Jpn J. Appl. Phys.* **27**, 1005–9.
Černák, M., and Hosokawa, T. (1989). *IEEE Trans. Elect. Insulation* **24**, 699–707.
Černák, M., and Hosokawa, T. (1991). *Phys. Rev.* A **43**, 1107–10.
Černák, M., Hosokawa, T., and Inoshima, M. (1990). *Appl. Phys. Lett.* **57**, 339–40.
Crichton, G. C., and Williams, W. T. (1983). Proc. 16th Int. Conf. on Phenomena in Ionised Gases, Dusseldorf (Eds W. Bötticher *et al.*), pp. 176–7 (Univ. Düsseldorf).
Gallimberti, I., and Marchesi, G. (1982). Proc. 7th Int. Conf. on Gas Discharges, London, pp. 136–9 (Peter Perelgrinus).
Goldman, M., and Goldman, A. (1978). *In* 'Gaseous Electronics' (Eds M. E. Hirsch and H. S. Oskam), Chap. 4 (Academic: New York).
Golinski, J., and Grudzinski, J. (1986). *J. Phys.* D **19**, 1497–505.
Graf, D. (1979). Proc. 3rd Int. Symp. on High Voltage Engineering, Milan, Paper 53.04.
Graf, D. (1980). Proc. 6th Int. Conf. on Gas Discharges, Edinburgh (Ed. B. F. Hampton), pp. 142–5 (IEE: London).
Guile, A. E., Dimoff, K., and Vijh, A. K. (1983). *Proc. IEE* A **130**, 379–86.
Hauschild, W. (1985). 17th Int. Conf. on Phenomena in Ionised Gases, Budapest (Eds J. S. Bakos and Z. Sorlei), pp. 52–61 (Hungarian Acad. Sci.).
Hodges, R. V., Varney, R. N., and Riley, J. F. (1985). *Phys. Rev.* A **31**, 2610–20.
Hosokawa, T., Kondo, Y., and Miyoshi, T. (1969). *Elect. Engineering in Japan* **89**, 120–7.
Hosokawa, T., Kondo, Y., and Miyoshi, T. (1970). *Elect. Engineering in Japan* **90**, 151–8.
Ikuta, N., and Kondo, K. (1976). *IEE Conf. Publ.* **145**, 227–30.
Inoshima, M., Černák, M., and Hosokawa, T. (1990). *Jpn J. Appl. Phys.* **29**, 1165–72.
Kunhardt, E. E., and Tzeng, Y. (1988). *Phys. Rev.* A **38**, 1410–21.

Loeb, L. B. (1965). 'Electrical Coronas: Their Basic Physical Mechanism' (Univ. California Press).
McAllister, I. W., Crichton, G. C., and Brengsbo, E. (1979). *J. Appl. Phys.* **50**, 6797–805.
Miyoshi, Y., Hosokawa, T., and Sakai, O. (1964). Nagoya Inst. Technology Bull. No. 16, 235–7.
Morrow, R. (1985*a*). *Phys. Rev.* A **32**, 1799–809.
Morrow, R. (1985*b*). *Phys. Rev.* A **32**, 3821–4.
Ogasawara, M. (1966). *J. Phys. Soc. Jpn* **21**, 2360–71.
Poli, E. (1982). Proc. 7th Int. Conf. on Gas Discharges, London, pp. 132–5 (Peter Perelgrinus).
Raether, H. (1964). 'Electron Avalanches and Breakdown in Gases' (Butterworths: London).
Salasoo, L., Nelson, J. K., Schwabe, R. J., and Snaddon, R. W. L. (1985). *J. Appl. Phys.* **58**, 2949–57.
Scott, D. A., and Haddad, G. N. (1987). *J. Phys.* D **20**, 1039–44.
Scott, R. P., and Fowler, R. G. (1977). *Phys. Fluids* **20**, 27–31.
Shimozuma, M., and Tagashira, H. (1981). *J. Phys.* D **14**, 1783–9.
Trichel, G. W. (1938). *Phys. Rev.* **54**, 1039–44.
Turner, R. (1981). *J. Appl. Phys.* **52**, 601–92.
Ushita, T., Ikuta, N., and Yatsuzuka, M. (1967). Bull. Faculty of Engineering of Tokushima University No. 4, 89–100.
Ushita, T., Ikuta, N., and Yatsuzuka, M. (1968). *Elect. Engineering in Japan* **88**, 45–50.

Manuscript received 1 July, accepted 5 December 1991